μ-ANALYSIS AND SYNTHESIS OF A MAGNETIC SUSPENSION SYSTEM CONSIDERING STRUCTURED UNCERTAINTIES

Toru Namerikawa[1], Masayuki Fujita[2], and Fumio Matsumura[1]

[1] Department of Electrical and Computer Engineering, Kanazawa University
2-40-20 Kodatsuno, Kanazawa 920, Japan
e-mail: toru@t.kanazawa-u.ac.jp
[2] School of Information Science, Japan Advanced Institute of Science and Technology
1-1 Asahidai, Tatsunokuchi, Ishikawa 923-12, Japan
e-mail: fujita@jaist.ac.jp

SUMMARY

This paper deals with modeling, structured uncertainties, μ-analysis and synthesis of a magnetic suspension system. First we derive a nominal model of the plant and consider its structured uncertainties, e.g., linearization error, parametric uncertainties, and neglected dynamics. Then we set the interconnection structure which includes the above structurally represented uncertainties. Next we design a robust μ controller which achieves robust performance conditions using the structured singular value μ. Finally we evaluate the proposed interconnection structure and verify robustness and performance of the designed μ controller by experiments.

INTRODUCTION

Magnetic suspension systems can suspend objects without any contact. Increasing use of this technology is now made for various industrial purposes, and it has already been applied to magnetically levitated vehicles, magnetic bearings, etc. [1,2]. Recent overviews and advances in this field are shown in [3]. Since magnetic suspension systems are essentially unstable, a feedback control is indispensable. The problem is that model uncertainties and perturbations often make the systems unstable.

In the robust control of magnetic suspension technology field, these uncertainties have been treated as exogenous disturbances, and unstructured uncertainties [4], however, both uncertainty descriptions caused the conservative analytic results for robust stability/performance tests. In [5], parameter perturbations were considered, and the model uncertainties were described structurally, but the unmodeled dynamics written as unstructured uncertainties is not fully discussed.

In this paper, our novelty is to propose the model and structured uncertainty description of a magnetic suspension system, which contains less conservativeness for robust stability/performance analysis. This is concerned with how to construct a set of plant models. We consider the parametric uncertainties and unmodeled dynamics and linearization error. These uncertainties are structurally described by real/complex numbers/matrices, and for robustness analysis, we employ

the mixed structured singular value (mixed μ) test [6] to reduce conservativeness. Finally we evaluate the proposed model and the robustness and performance of a designed μ controller by several experimental results.

MAGNETIC SUSPENSION SYSTEM

In this section, we derive an ideal model of the system based on physical laws and several assumptions.

Construction

Consider the electromagnetic suspension system shown schematically in Fig. 1. An electromagnet is located at the top of the experimental systems.

The control problem is to levitate the iron ball stably utilizing the electromagnetic force, where a mass M of the iron ball is 1.04kg, and steady state gap X is 5mm. Note that this simple electromagnetic suspension system is unstable, thus feedback control is dispensable. As a gap sensor, a standard induction probe of eddy current type is placed below the ball.

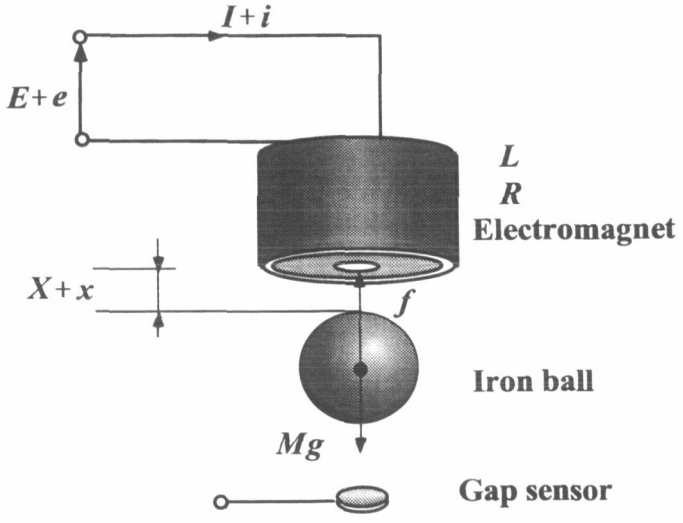

Figure 1: Magnetic Suspension System (M.S.S.)

Mathematical Model

In order to derive a model of the system by physical laws, we introduce following assumptions [1, 2, 4].

[A1] Magnetic flux density and magnetic field do not have any hysteresis, and they are not saturated.

[A2] There is no leakage flux in the magnetic circuit.

[A3] Magnetic permeability of the electromagnet is infinity.

[A4] Eddy current in the magnetic pole can be neglected.

[A5] Coil inductance is constant around the operating point, and an electromotive force due to a motion of the iron ball can be neglected.

These assumptions are almost essential to model this system. Under these assumptions, we derived equations of the motion, the electromagnetic force, and the electric circuit as

$$M\frac{d^2x}{dt^2} = Mg - f, \tag{1}$$

$$f = k\left(\frac{I+i}{X+x+x_0}\right)^2, \tag{2}$$

$$L\frac{di}{dt} + R(I+i) = E + e, \tag{3}$$

where M is a mass of the iron ball, X is a steady gap between the electromagnet (EM) and the iron ball, x is a deviation from X, I is a steady current, i is a deviation from I, E is a steady voltage, e is a deviation from E, f is EM force, k, x_0 are coefficients of f, L is an inductance of EM, and R is a resistance of EM.

Next we linearize the electromagnetic force (2) around the operating point by the Taylor series expansion as

$$f = k\left(\frac{I}{X+x_0}\right)^2 - K_x x + K_i i, \tag{4}$$

$$K_x = 2kI^2/(X+x_0)^3, \quad K_i = 2kI/(X+x_0)^2.$$

From equations (1), (3), (4) and the steady state equations: $Mg = k\left(\frac{I}{X+x_0}\right)^2, RI = E,$ the nominal block diagram of the magnetic suspension system is represented in Fig. 2. With the nominal model parameters in Table 1, a transfer function of the nominal model is given by

$$G_{nom}(s) = \frac{-28.9}{(s+28.8)(s+78.0)(s-78.0)}. \tag{5}$$

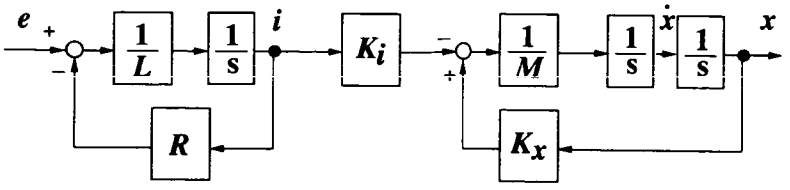

Figure 2: Nominal linear model for M.S.S.

Table 1: Model Parameters

Parameter	Nominal Value	Unit
M	1.04	[kg]
X	5.00 $\times 10^{-3}$	[m]
I	0.789	[A]
k	1.71 $\times 10^{-4}$	$[Nm^2/A^2]$
x_0	-1.80 $\times 10^{-3}$	[m]
K_x	6.27 $\times 10^{3}$	$[N/m]$
K_i	25.7 $\times 10^{-4}$	$[N/A]$
L	0.859	[H]
R	24.76	$[\Omega]$

STRUCTURED UNCERTAINTIES

Note that the model of the plant in Fig. 2 was introduced based on several assumptions and approximations. This model cannot always express the exact behavior of the real plant. We consider model uncertainties between the real physical system and the ideal nominal model, and make a set of plant models. Generally, it is well known that the following items are serious uncertainties [7] and we discuss them in the following:

- linearization error
- parametric uncertainty
- unmodeled dynamics

Linearization Error

There should be model uncertainties caused by linearization of the electromagnetic force around the operating point. In Fig. 3, the current-force (*i-f*) curve at X = 5.0mm is plotted in the upper figure, and gap-force (*x - f*) curve at *I* = 1.15A is in the lower figure, where O denotes measured experimental data at each point, and the solid lines show the determined current-force curve and gap-force curve. The dashed straight lines indicate tangents of each curve at the operating points. These inclinations of tangents are employed as K_i and K_x, respectively. The dash-dot straight lines are sectors of the linearization errors. These data were measured five times at each point. From Fig. 3, the perturbations between tangents and curves become bigger if the operating points move from the original points. These errors were caused by linearization. Here we employ sector bounds to account for linearization error, and describe K_i and K_x as

$$K_i = K_{i0} + k_i\delta_i, \quad \delta_i \in [-1, 1], \tag{6}$$

$$K_x = K_{x0} + k_x\delta_x, \quad \delta_x \in [-1, 1], \tag{7}$$

where K_{i0} and K_{x0} are nominal values, k_i and k_x are weights of uncertainties.

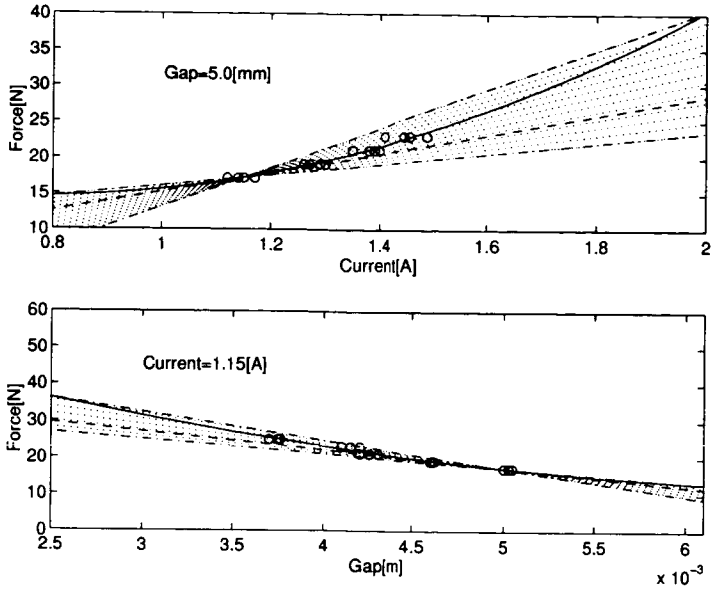

Figure 3: Current-Force Curve and Gap-Force Curve

Parametric Uncertainty

We had better consider the perturbation of a mass of the iron ball M against intentional change of the mass and against unexpected exogenous force disturbances. Hence, with a perturbation we describe it as

$$M = M_0 + k_M \delta_M, \quad \delta_M \in [-1, 1], \tag{8}$$

where, M_0 is the nominal value, and k_M is magnitude of perturbation.

Unmodeled Dynamics

In this section, we discuss the dynamics of the electromagnet which can be represented as $\frac{1}{Ls+R}$. Inductance L and resistance R of the electromagnet have frequency dependent characteristics. Also, measurements of these parameters are very sensitive. Nominal values of L, R are determined as averages of measurements under forcing at 10Hz. Figure 4 shows the experimental data of $\frac{1}{Ls+R}$, where the solid line indicates the nominal frequency response and the dashed lines indicate upper and lower bounds. The dynamics of electromagnet, $\frac{1}{Ls+R}$, are distributed in a frequency dependent belt. Furthermore, if the frequency of the input signal changes, this belt becomes broad. We treat the width of this belt in Fig. 4 as an unstructured uncertainty as below.

$$\frac{1}{Ls+R} = \frac{1}{L_0 s + R_0} + w_i(s)\Delta_i(s), \quad |\Delta_i(jw)| \leq 1. \tag{9}$$

where L_0 and R_0 are the nominal values of L and R, respectively, and $w_i(s) = d_w + c_w(sI_m - A_w)^{-1}b_w$ is a weight of uncertainty. The magnitude of weight $w_i(s)$ is determined as one half of a width of the belt in Fig. 4.

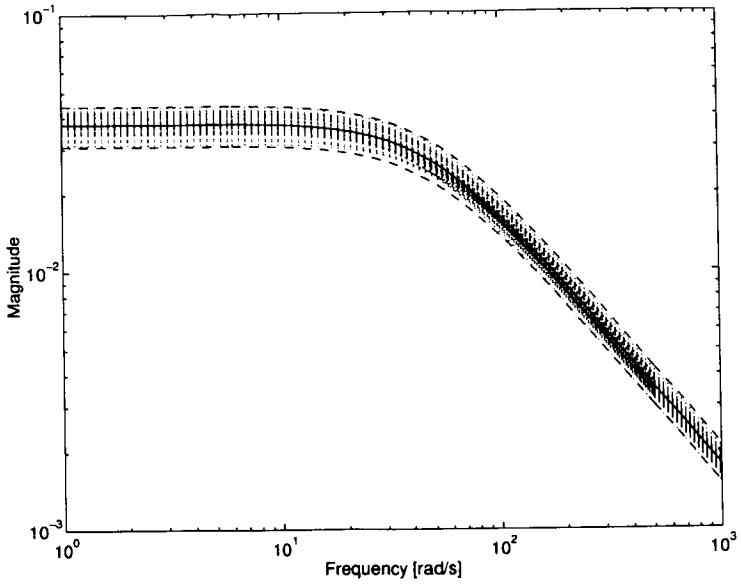

Figure 4: Frequency responses of $\frac{1}{Ls+R}$

Set of Plant Models

We take into account the above three types of uncertainties, and reconstruct the block diagram of the system in Fig. 2. The obtained set of models which includes the above uncertainties is shown in Fig. 5.

μ-ANALYSIS AND SYNTHESIS

Quantization of Uncertainties

In this section, we quantify uncertainties and make a real set of plant models.

Change of the Operating Point

We consider a structurally represented uncertainty caused by a change of the operation point. In this system, the operating point is characterized by a steady state gap X $\{X \mid 3.8 \leq X \leq 6.2\}$.

Perturbation of K_i and K_x

Change of the operating point X causes the other perturbations of parameters, K_i and K_x. In this case, parameters K_i and K_x perturb as $14.1 \leq K_i \leq 37.3$, $5.38 \times 10^3 \leq K_w \leq 7.16 \times 10^3$ $(3.8 \leq X \leq 6.2)$. Then we describe K_i and K_x as below.

$$K_i = 25.7 + 11.6 \cdot \delta_i, \quad \delta_i \in [-1, 1], \tag{10}$$

$$K_x = 6.27 \times 10^3 + 8.90 \times 10^2 \cdot \delta_x, \quad \delta_x \in [-1, 1]. \tag{11}$$

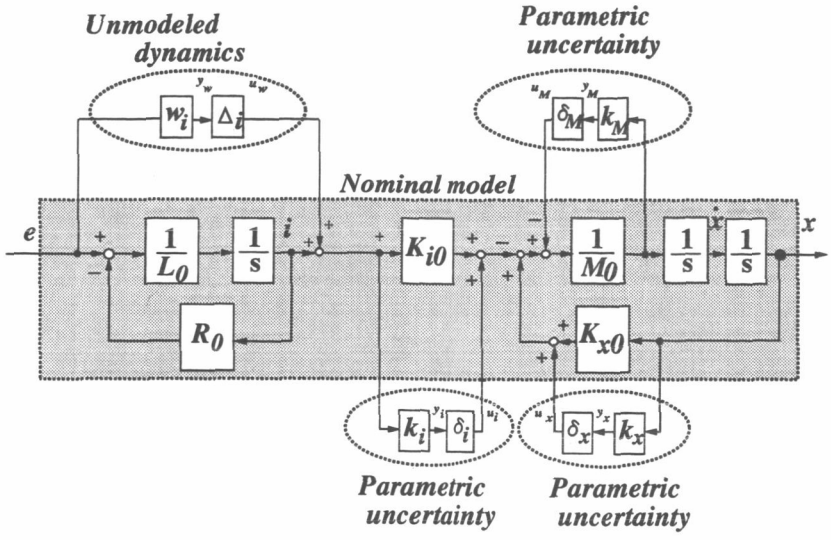

Figure 5: Set of Plant Models with Uncertainties

Dynamical uncertainties

An uncertainty in the electromagnet, $\frac{1}{Ls+R}$, should be also considered. We set the parametric uncertainty of L and R as $0.782 \leq L \leq 0.936$ (9% perturbation) and $24.5 \leq R \leq 25.0$ (1% perturbation). In addition to the above parametric perturbation, we should take into account unmodeled dynamics in the high frequency range. Using an FFT analyzer, we measured them. Finally, we decided a set of electromagnetic dynamics, $\frac{1}{Ls+R}$, as

$$\frac{1}{Ls+R} = \frac{1}{0.859s+24.8} + \frac{1.28 \times 10^{-3}(s+3.20)(s+900)}{(s+25.8)(s+31.4)}\Delta_i(s), \quad |\Delta_i(jw)| \leq 1. \tag{12}$$

From the above discussion in these three subsections, the final quantity of uncertainties are selected in Table 2, where a 7% perturbation of mass M is considered in this case.

Table 2: Quantity of uncertainties

	Value		Value
k_i	11.6	k_x	8.90×10^2
k_M	7.25×10^{-2}	$w_i(s)$	$\frac{1.28\times10^{-3}(s+3.20)(s+900)}{(s+25.8)(s+31.4)}$

Design

Utilizing the structured singular value μ [8, 9], we design the controller which achieves robust performance against various types of uncertainties.

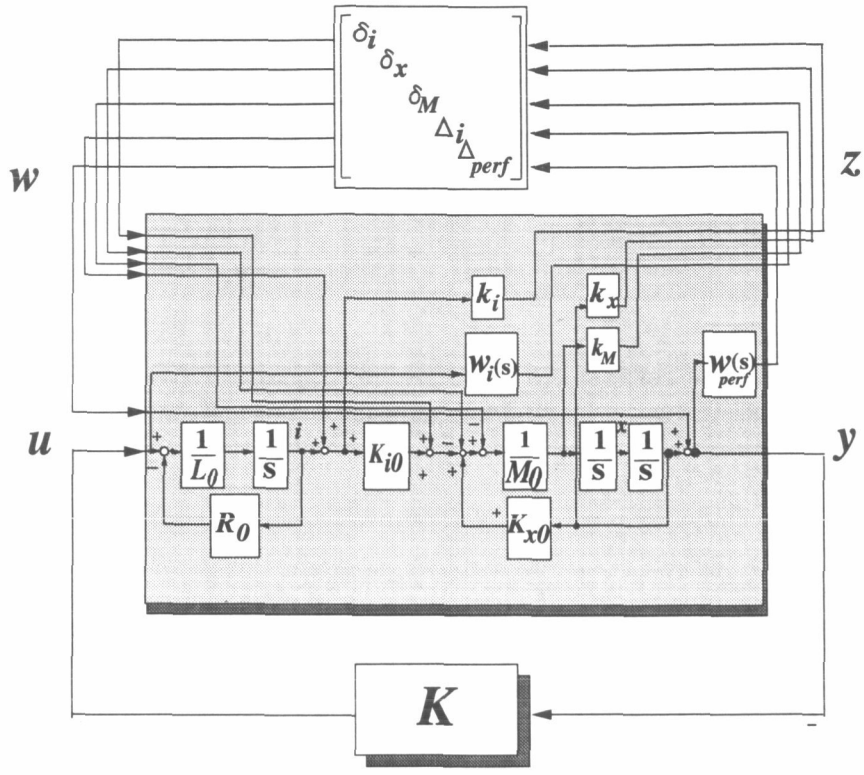

Figure 6: Interconnection Structure

We construct an interconnection structure by LFT representation in Fig. 6, where W_{perf} is a performance specification and also is a weight for a sensitivity function $S := (I + G_{nom}K)^{-1}$. W_{perf} is given by a following equation, and its frequency response is shown in Fig. 7.

$$W_{perf}(s) = \frac{100}{1 + s/0.1}. \tag{13}$$

Next, for the robust performance synthesis, we define the block structure Δ. The perturbation $\Delta(s)$ belongs to the bounded subset

$$\mathbf{B\Delta} := \{\Delta(s) \in \mathbf{\Delta} | \bar{\sigma}(\Delta(j\omega)) < 1\}, \tag{14}$$

where Δ is given by

$$\mathbf{\Delta} := \{\mathrm{diag}[\delta_i, \delta_x, \delta_M, \Delta_i, \Delta_{perf}] : \quad \delta_i, \delta_x, \delta_M \in \mathbf{R}, \Delta_i, \Delta_{perf} \in \mathbf{C}\}. \tag{15}$$

The structured singular value $\mu_\Delta(M)$ is defined for matrices $M \in \mathbf{C}^{n \times n}$ with the block structure Δ as

$$\mu_{\mathbf{\Delta}}(M) := \frac{1}{\min\{\bar{\sigma}(\Delta) : \Delta \in \mathbf{\Delta}, \det(I - M\Delta) = 0\}} \tag{16}$$

unless no $\Delta \in \mathbf{\Delta}$ makes $(I - M\Delta)$ singular, in which case $\mu_\Delta(M) := 0$.

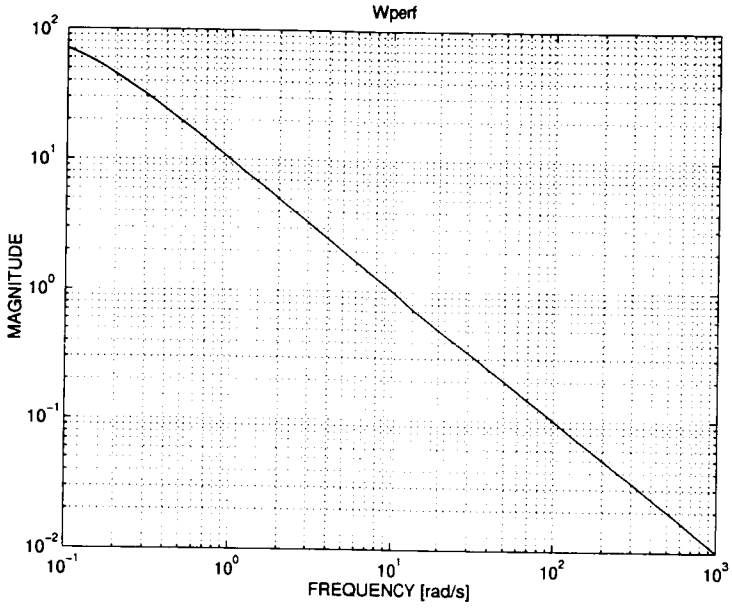

Figure 7: Weighting Function W_{perf}

We then have:
- The closed loop system will have robust performance, i.e., it will be robustly stable and

$$\sup_{\omega \in R} \mu_{\Delta}[F_l(P(j\omega), K(j\omega))(j\omega)] < 1. \tag{17}$$

We apply standard D - K iteration to find the sub-optimal μ controller for the system. We thus iteratively solve the following problem:

$$\sup_{\omega \in R} \inf_{D(\omega)} \{\bar{\sigma}(D(j\omega)F_l(P(j\omega), K(j\omega))(j\omega)D^{-1}(j\omega))\} < 1. \tag{18}$$

After the 3rd iteration, we obtained a controller *K(s)*, where the supremum of μ_{Δ} [F_l(P,*K*)] is 0.9766. Final scaling matrix *D(s)* has 12 states, then *K(s)* has 30 states. We employ the Hankel norm approximation technique to calculate the reduced order system of *K(s)*. Final balanced controller *K(s)* is as follows, and its bode diagram is shown in Fig. 8. The supremum of the $\mu_{\Delta}[F_l(P, \hat{K})]$ is also 0.9766.

$$\begin{aligned}
\hat{K}(s) &= \frac{3.27 \times 10^{10} \times (s+486+885i)(s+486-885i)}{(s+1740)(s+949+1320i)(s+949-1319i)} \\
&\times \frac{(s+389+626i)(s+389-626i)(s+335)(s+79.1)(s+29.5)}{(s+472+794i)(s+472-794i)(s+391+599i)(s+391-599i)(s+348)} \\
&\times \frac{(s+14.7)(s+4.86)(s+2.63)(s+0.175)(s+0.114)}{(s+8.16)(s+2.66)(s+0.210)(s+0.127)(s+0.0778)}
\end{aligned} \tag{19}$$

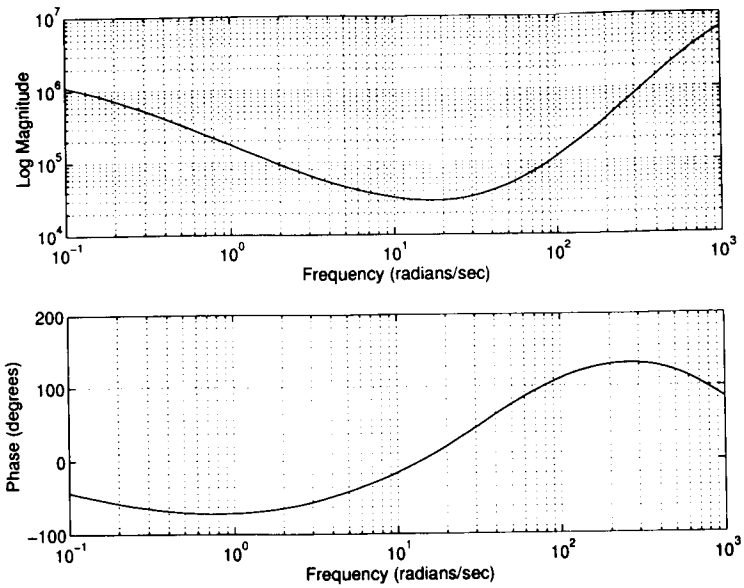

Figure 8: Final Controller $\hat{K}(s)$

A calculated upper bound and lower bound of $\mu_{\Delta}[F_l(P, \hat{K})]$with the controller $\hat{K}(s)$ is shown in Fig. 9., where the two solid lines respectively show upper and lower bounds of μ and the dashed line shows the maximum singular value of $(D(j\omega)F_l(P(j\omega), \hat{K}(j\omega))(j\omega)D^{-1}(j\omega))$.

A peak value of the upper bound of μ is less than 1, then the closed-loop system with considered uncertainties achieves the robust performance condition. This result shows guarantees robust performance against uncertainties caused by a change of operating point $\{X \mid 3.8 \leq X \leq 6.2\}$.

EXPERIMENTAL EVALUATION

In order to evaluate the design process, we implement the obtained controller $\hat{K}(s)$ via a digital controller, and carry out experiments. The sampling period of the controller is 95μs, and a well known Tustin transform was employed for discretization. All experimental results which show a position of the iron ball are shown in Fig. 10.

Evaluation of Nominal Performance

Step response of the position x of the iron ball at X = 5[mm] (nominal steady gap) is shown in Fig. 10(a), which indicates stable levitation with the controller $\hat{K}(s)$ at the nominal steady gap X = 5.0mm. The magnitude of the step-type disturbance is 22 N, which is twice as much as the steady state force. Since it is difficult to give disturbance forces to the iron ball directly, we add a pseudo-disturbance by applying a voltage signal to the control input signal. This figure shows that the nominal performance is fully achieved.

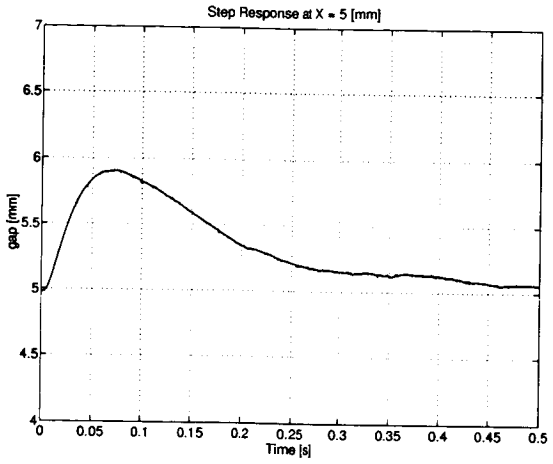

(a) Step Response at $X = 5$[mm]

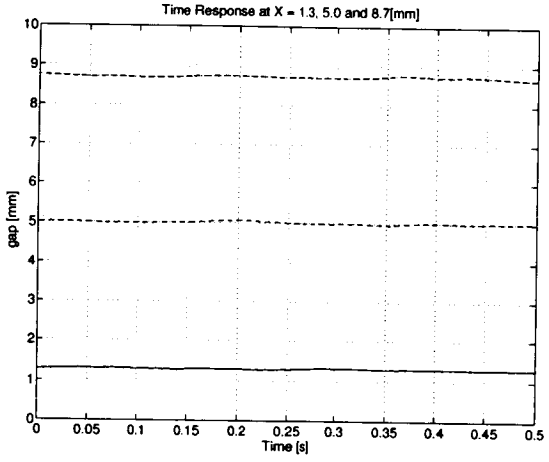

(b) Time Response at $X = 1.3,\ 5.0,\ 8.7$[mm]

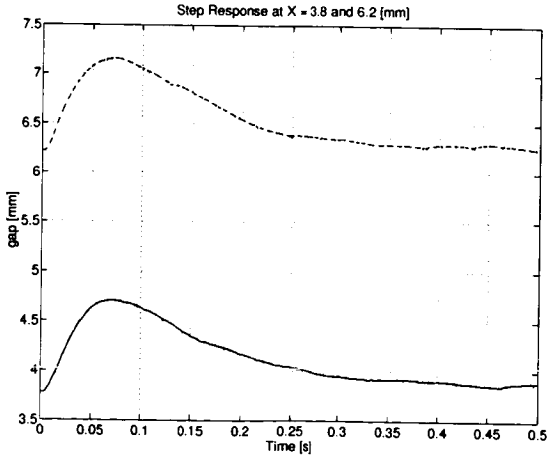

(c) Step Response at $X = 3.8,\ 6.2$[mm]

Figure 10: Experimental Results

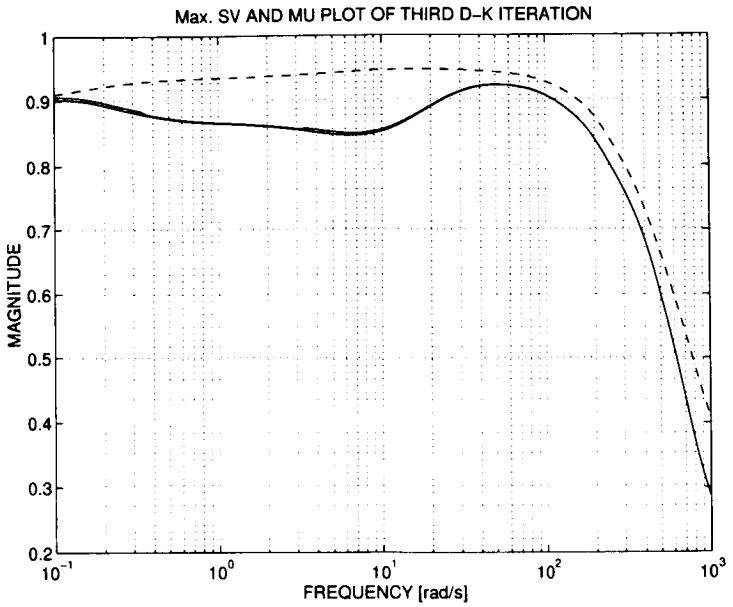

Figure 9: $\mu_{\Delta}[F_l(P,\hat{K})]$ and $\bar{\sigma}[DF_l(P,\hat{K})D^{-1}]$

Evaluation of Robust Stability

Time responses of the controllers $\hat{K}(s)$ are shown in Fig. 10(b), which indicate stable levitation at the steady state gaps $X = 1.3, 5.0, 8.7$ mm. These lines show that the robust stability against the perturbation of X $(1.3 \leq X \leq 8.7)$ is achieved. If we change the steady state gap X to less than $X = 1.3$, or greater than $X = 8.7$, then the system disappointingly becomes unstable.

Evaluation of Robust Performance

For the verification of the robust performance test, we measured time responses against a step-type external disturbance (22 N) at the steady state gaps $X = 3.8$, 6.2mm. Results are shown in Fig. 10(c).

From this result, it can be seen that the controller $\hat{K}(s)$ shows adequate performance comparing the response in Fig. 10(a). We have confirmed $\hat{K}(s)$ achieves robust performance against model perturbances caused by a change of operating point $\{X \mid 3.8 \leq X \leq 6.2\}$.

CONCLUSIONS

In this paper, we proposed a novel set of plant models for a magnetic suspension system considering structured uncertainties.

We transformed the obtained model to the LFT represented interconnection structure with the structured mixed uncertainty. Next we designed a robust controller by μ-analysis and synthesis which achieves robust performance criteria using the structured singular value μ. Finally we evaluated the proposed interconnection structure which contained the structured uncertainties, and also verified robustness and performance of the designed μ controller by experiments.

REFERENCES

[1] P. K. Sinha: *Electromagnetic Suspension: Dynamics and Control, IEE,* Peter Peregrinus, London, 1987.

[2] G. Schweitzer, et al.: *Active Magnetic Bearings,* Hochschulverlag AG an der ETH Zurich, 1994.

[3] F. Matsumura, Ed.: *Proc. of the Fifth Int. Symp. on Magnetic Bearings,* Kanazawa, Japan, Aug. 1996.

[4] M. Fujita, T. Namerikawa, et al.: "*μ*-Synthesis of an Electromagnetic Suspension System," *IEEE Trans. Automatic Control,* Vol. 40, No. 3, pp. 530-536, 1995.

[5] T. Sugie and M. Kawanishi: "Analysis and Design of Magnetic Levitation Systems Considering Physical Parameter Perturbations," *Trans. of ISCIE,* Vol. 8, No. 2, pp. 70-79, 1995.

[6] P. M. Young: " Controller Design with Real Parametric Uncertainty," *Int. J. of Control,* Vol. 65, No. 3, pp. 469-509, 1996.

[7] F. Paganini: *Sets and Constraints in the Analysis of Uncertain Systems,* Ph.D. Thesis, California Institute of Technology, 1996.

[8] G. J. Balas, J. C. Doyle, K. Glover, A. Packard, and R. Smith: *μ-Analysis and Synthesis Toolbox User's Guide*, MUSYN Inc. and Math Works, 1993.

[9] G. Stein and J. C. Doyle: "Beyond Singular Values and Loop Shapes," *J. Guidance,* Vol. 14, No. 1, pp. 5-16, 1991.